

# 3D numerical modeling of a landslide in Switzerland

S. Command & F. Geiser

*GeoMod consulting engineers, Lausanne, Switzerland*

L. Tacher

*Geolep-EPFL, Swiss Federal Institute of Technology, Lausanne*

**ABSTRACT:** A fully coupled elastoplastic 3D finite element approach applied to a large landslide analysis is described in this paper. First, a hydrogeological model has been adopted by the engineers. Then, a flow-only computation, including geology and transient hydraulic conditions, has been carried out with Feflow. Finally, resulting hydraulic boundary conditions have been introduced in a fully coupled transient finite element model (Z\_Soil 2004) in order to reproduce the hydro-mechanical aspects of the landslide over a crisis period of about two years (1993-1995). After a careful comparison between computed and observed pressures and displacements, the model has been used in order to evaluate the impact of constructive solutions, such as drainage or filling, on the behavior of the landslide.

## 1 INTRODUCTION

Located in the Swiss Prealps, a landslide covering a surface of about 2.1 km x 0.5 km (Fig. 1) crosses two regional tourist roads. Important displacements have been observed there for over 150 years, and dating methods show that the landslide has been active for millennia.

Sliding velocities vary in space and time. They locally reach 4 meters per year during crisis periods in the downhill part of the landslide. This critical zone is referred to as the + / ++ zone, where local velocities reach their peak (see Fig. 3).

A main sliding surface has been identified at a mean depth of 40 to 80 m, where boreholes show groundwater excess pressures that are also present within the sliding mass.

A first attempt to slow down the most active part of the slide by drainage wells at the top of the ++ zone has been carried out in 1994-1995.

## 2 GEOLOGICAL MODELLING

A 3-D structural geological model synthesizing all available data (boreholes, geophysics, field observations) is built serving to design the stabilization project. It is also the shape on which are based finite elements meshes for hydrogeological and hydromechanical numerical modelling.

La Frasse landslide slides along a slope oriented NW to SE, down to the Grande Eau river which erodes its toe continuously (Fig. 1). In the area, the

main geological structure is a pinched syncline of Mesozoic (Triassic dolomites, Malm limestones) and Tertiary rocks (Eocene siltstones and flysch). The syncline axe is orientated SW-NE, according the global alpine structures. Only a part of the Tertiary flysch (sandstones and clay schists) is sliding.

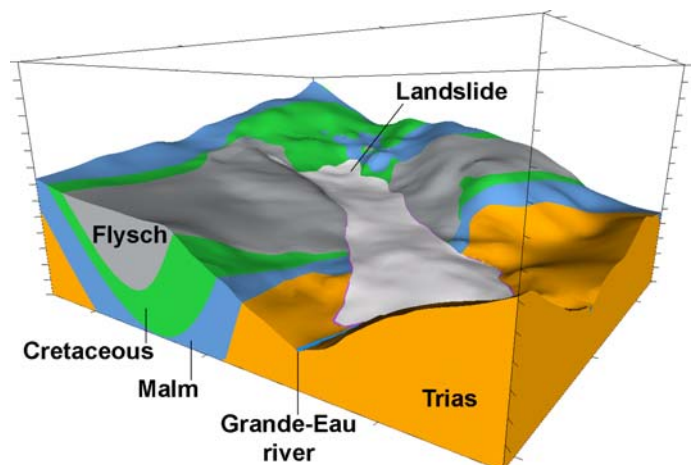


Figure 1. La Frasse 3D geological model. View from S-E.

## 3 HYDROGEOLOGICAL MODELLING

Groundwater flows and pressures are simulated by 3-D finite element transient modelling (Feflow). Calculated pressure fields are then exported toward the geomechanical models. The two major difficulties to address are the infiltration conditions and the heterogeneity of the medium.

*Infiltration conditions* : Although groundwater is recognized to be the cause of sliding, the correlation of acceleration phases with gross rainfall is rather poor. However, a correlation exists with an accurate infiltration computation (COUP model, Jansson) weighted up to two years before the day of calculation. This means that events of the past intervene in the present behaviour. Indeed, the hydraulic balance of the system (about 5000 m<sup>3</sup>/d) shows that about 1/3 of the inflow is supplied by superficial infiltration and 2/3 by the borders of the landslide.

*Heterogeneity* : Sliding adds heterogeneity to the original one due to the flysch, leading to a network of more permeable structures (1E-2 m/s or more) in a matrix of shales (1E-7 m/s). Pumping tests show that the connectivity of the permeable structures is higher parallel to the landslide and reaches hundreds of meters; the width of these structures is of the order of 10 m, which is a determining value for the spacing of future drains or wells.

In the model, heterogeneity is underestimated and represented by a system of channels in the permeability field. As a consequence, results must be read at the landside scale rather than at a local scale. They show that, in accordance with observations, hydraulic heads vary in time from some meters in the upper part of the landslide to some tens of meters downhill (Fig. 2a and 2b).

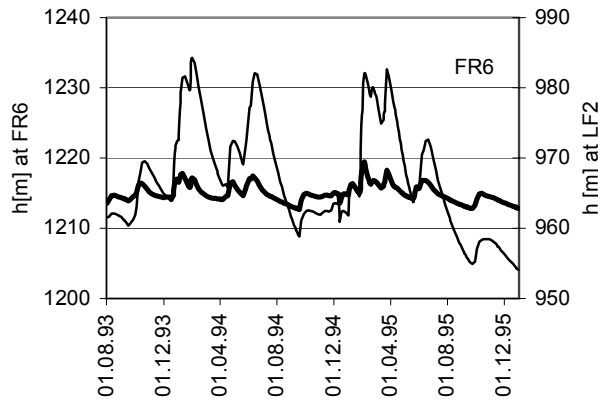


Figure 2a. Calculated hydraulic head at piezometers FR6 (thick line) and LF2 (thin line).

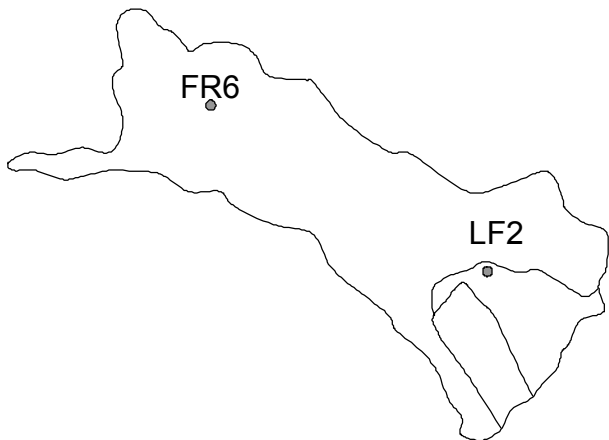


Figure 2b. Localisation of piezometers FR6 and LF2.

## 4 HYDROMECHANICAL MODELLING

### 4.1 Introduction

A 30'000 elements finite element mesh is used in order to perform the hydromechanical analyses. It is depicted in Figure 3.

More than 350 different calculations have been conducted (including parametric studies, constructive solutions introduction, ...), each of them running on a P4 computer in about 10 to 15 hours (nonlinear transient analysis on 320 steps).

Pressure boundary conditions are interpolated from the Feflow model. From the mechanical point of view, the bedrock located under the flysch is considered fixed. The interaction of the bottom zone of the landslide with the river is modeled through a system of surface loads, evolving in space and time.

Material parameters are given in Table 1. They are based on a series of laboratory and in situ tests. Drucker-Prager and Cap models are the elastoplastic constitutive laws used here.

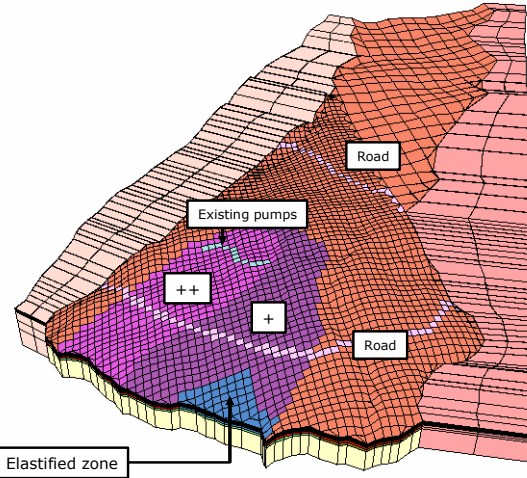


Figure 3. Hydromechanical FE mesh (30'000 B8 elements).

Table 1. Material parameters.

	Parameter	Unit	Above sliding plane	Sliding plane	Below sliding plane
Identification	Unit weight, $\gamma$	kN/m <sup>3</sup>	19.9	19.9	21.3
	Void ratio, $e_0$	-	0.4	0.4	0.3
	Permeability, K	m/s	7 e-7 to 2 e-5	7 e-7	7 e-7 to 1.5 e-5
Elasticity	Young's modulus, E	MPa	80	80	100
	Poisson ratio, $\nu$	-	0.3	0.3	0.3
Plasticity	Friction angle, $\phi$	°	30	25	33
	Cohesion, c	kPa	5 to 20	2	30
	Dilatance angle, $\psi$	°	30	25	33
	Plastic compressibility, $\lambda$	-	-	0.07	-
	OCR	-	-	Normal	-

## 4.2 Displacement results

The study concentrates on the period between August 1993 and December 1995, as a very well documented crisis happened in 1993-1994, yielding metric horizontal displacements at the bottom road (RC 705).

Figures 4-6 illustrate the computed displacement field at the end of the transient analysis. Their spatial distribution corresponds to the in situ measured displacement field including a crisis period, as Figure 6 shows.

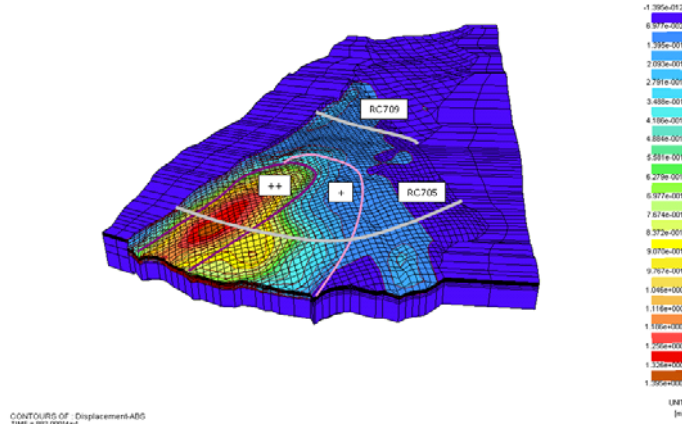


Figure 4. Absolute displacements from aug-93 till dec-95, 3D view.

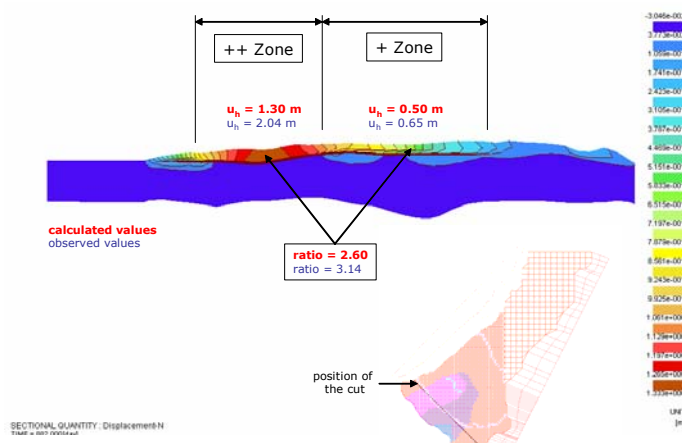


Figure 5a. Absolute displacements from aug-93 till dec-95, 2D cut along the main road crossing the landslide (RC 705).

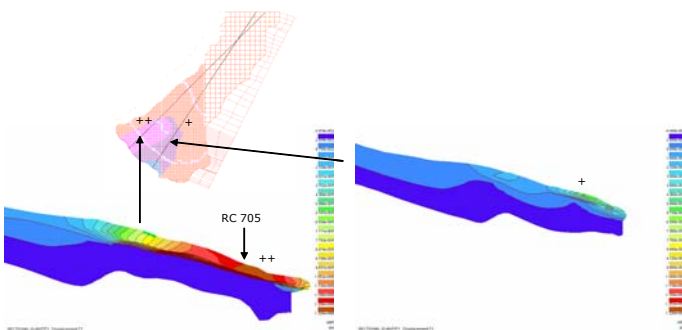


Figure 5b. Absolute displacements from aug-93 till dec-95, 2D cuts across + and ++ zones.

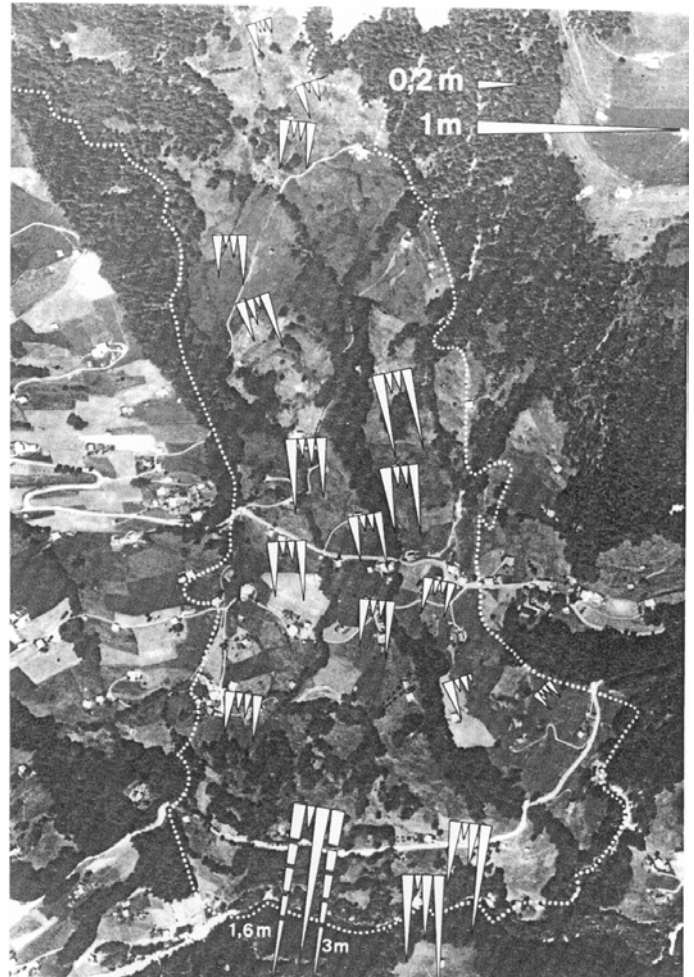


Figure 6. Observed displacements for 4 periods (between 1957 and 1982) (Duti).

## 4.3 Effect of pumping

In winter 94-95, an attempt to slow down the downhill part of the landslide has been undertaken. A pumping platform has been constructed at the top of the ++ zone (see Figure 3, “existing pumps”). The influence of the drainage wells and pumps at the top of ++ zone in winter 1994 can also be evaluated by the numerical model. Figure 7 illustrates the pore-water pressure drop that takes place in the model when the pumps are switched on.

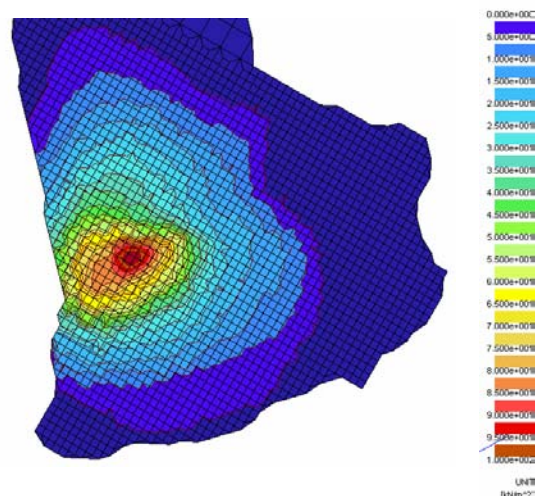


Figure 7. Pressure drop when the pumps are switched on in winter 1994-1995.

This effect on the pore pressure field has a great incidence on subsequent displacements. Looking at Figure 8, where observed and computed horizontal displacement histories at the RC 705 are compared, the drainage influence can be clearly identified for a second crisis, as velocities drop significantly in the ++ zone (ratio of 12 to 14), and less in the + zone (ratio of 3).

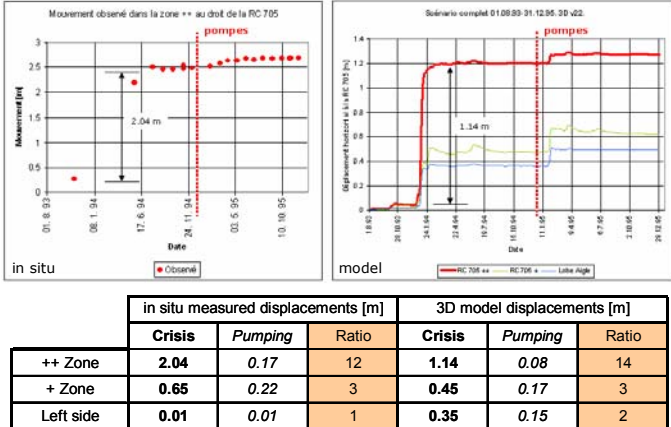


Figure 8. Comparison between computed and observed values before and after the construction of the pumping platform.

#### 4.4 Performance of the model

On the one hand, the comparison between observed and computed horizontal displacements shows a good agreement qualitatively (see Fig. 8). On the other hand, the model underestimates the in situ displacements by a factor of about two.

To some extent, this underestimation can be explained by the continuous nature of our model, as no sliding interfaces have been introduced in the mesh.

However, the global history of spatial displacements of the landslide is reproduced satisfactorily (modeled ratios before/after pumping are in good agreement with measured values), and the model is now ready to estimate the influence of constructive solutions on its behavior.

### 5 CONSTRUCTIVE SOLUTIONS

Two families of constructive solutions to slow down the landslide are analyzed:

- reinforcement of the landslide's toe through the construction of a concrete or earth filling in the Grande Eau river
- drawdown of pore-water pressures at the sliding surface through the construction of a drainage tunnel (or a pumping wells platform) across the landslide

#### 5.1 Grande Eau Filling

A 2D (see mesh, Fig. 9) parametrical study on a cut in the ++ zone has allowed us to evaluate the influ-

ence of the height of a filling placed in the Grande Eau area, where the landslide is eroded continuously by the river. Displacements drop quite significantly in the vicinity of the filling, but its efficiency drops very fast as soon as displacements above the RC 705 road are considered.

This can also be noticed on Figure 10, where cases with and without filling are considered. The landslide's motion is clearly slowed down by the filling, but its tendency to climb above the filling is also noticeable.

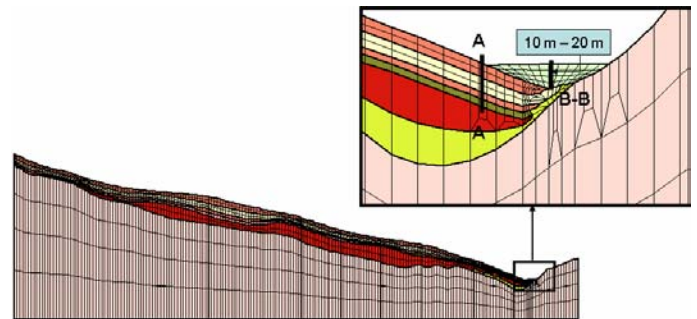


Figure 9: 2D model for the parametrical study of the filling.

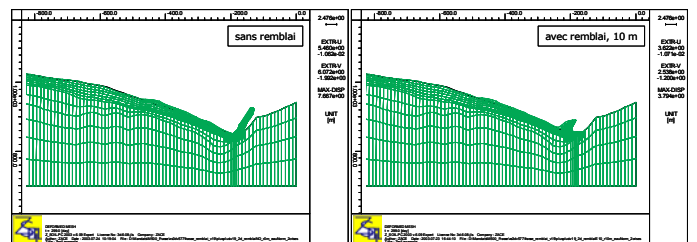


Figure 10. Deformed mesh in the ++ zone (left without filling, right with 10 m filling, same amplification factor = 3.75).

3D analyses of the filling's influence have also been performed, confirming the facts noticed on the 2D analyses: limited spatial efficiency and tendency to "climb" above the filling. Moreover, Figure 11 shows that the landslide also has a tendency to try to circumvent the filling, especially if subsequent crises follow the first one that we studied.

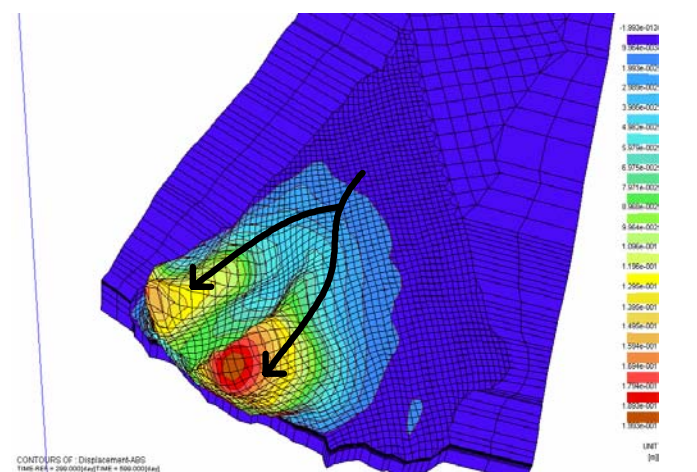


Figure 11. Horizontal displacement map. Effect of a second crisis following the 93-94 one.

## 5.2 Drainage systems

Hydraulic heads can vary in time to tens of meters in the downhill part of the landslide. Under these conditions, efficient stabilization works may consist in a series of wells or sub vertical drains drilled from a gallery in the substratum, located at the top of the most active area of the landslide, to draw down and stabilize hydraulic heads.

The studied drainage systems are modelled by imposing additional head boundary conditions.

## 5.3 Comparison

Figure 12 gives the horizontal displacement maps at the end of the 93-95 period for four cases:

- Reference case (top left)
- 10 m filling (bottom left)
- Existing pumping “as for now” (top right)
- Drainage tunnel (bottom right)

It is quite obvious that the only constructive solution which prevent metric displacements to develop at the bottom of the landslide under crisis conditions is the drainage tunnel, active on the whole landslide’s width (a similar observation can be made on the projected pumping solution, as it possesses the same implantation as the gallery).

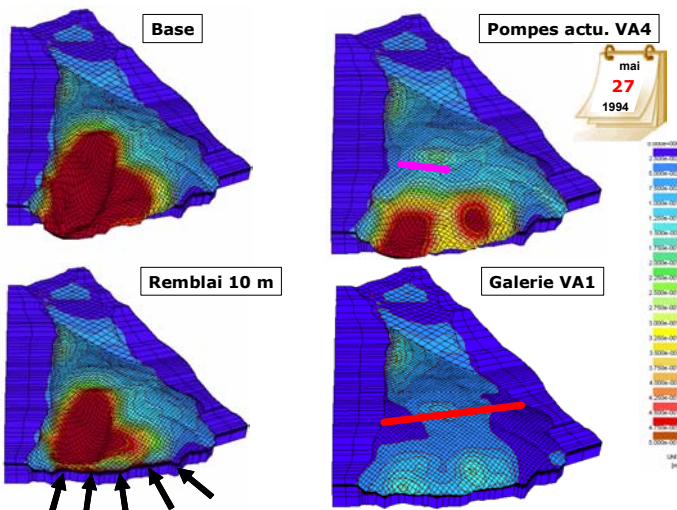


Figure 12. Comparison of different constructive solutions, displacement field at the end of the analysis (dec-95).

The efficiency of each solution is given in Figure 13 with respect to the distance to the Grande Eau river. As expected, the filling solution is only efficient in the vicinity of the river. The pumping “as for now” method reaches its peak performance near the pumping platform but would fail to be really helpful in the downhill zone, if a new crisis period happened. Again, the two most efficient solutions are the drainage tunnel and the projected pumping that totally cross the landslide. A “super”-efficient

solution would be to continue the drainage tunnel uphill, yielding a drastic diminution of the projected displacements.

Finally, stability analyses have been performed for all cases, by progressively decreasing the friction angle and the cohesion of the different materials, until failure occurs. This gives another point of view on the efficiency of the different stabilization methods, confirming the supremacy of the drainage solutions (see Table 2).

## 6 CONCLUSIONS

A fully coupled hydromechanical elastoplastic 3D FE analysis has been conducted in order to reproduce the behavior of a large landslide located in the Swiss Alps.

Comparisons with in situ observations show that the model performs well and is able to predict the impact of constructive solutions on the future behavior of the landslide.

## ACKNOWLEDGEMENTS

The authors would like to thank the following institutions and companies for their confidence and their support:

- the Swiss Federal Office for Water and Geology- OFEG (MM. Lateltin and Raetzo),
- the “Service des eaux, sols et assainissements- SESA” (M. Matthey),
- the “Association for the study of La Frasse landslide”, grouping De Cérenville Géotechnique SA and Norbert Géologues-Conseils SA as well as two institutes of the Swiss Federal Institute of Technology-EPFL (LMS and GEOLEP).

## REFERENCES

- Feflow software, Groundwater modeling system, Wasy AG, Berlin.
- Z\_Soil 2004. User manual. Zace Services Ltd Report 1985-2004. Lausanne, Elmepress International.
- Duti 1986. Etude de site, le glissement de Cernnat-La Frasse. Analyse pluridisciplinaire. Ecole Polytechnique Fédérale de Lausanne.

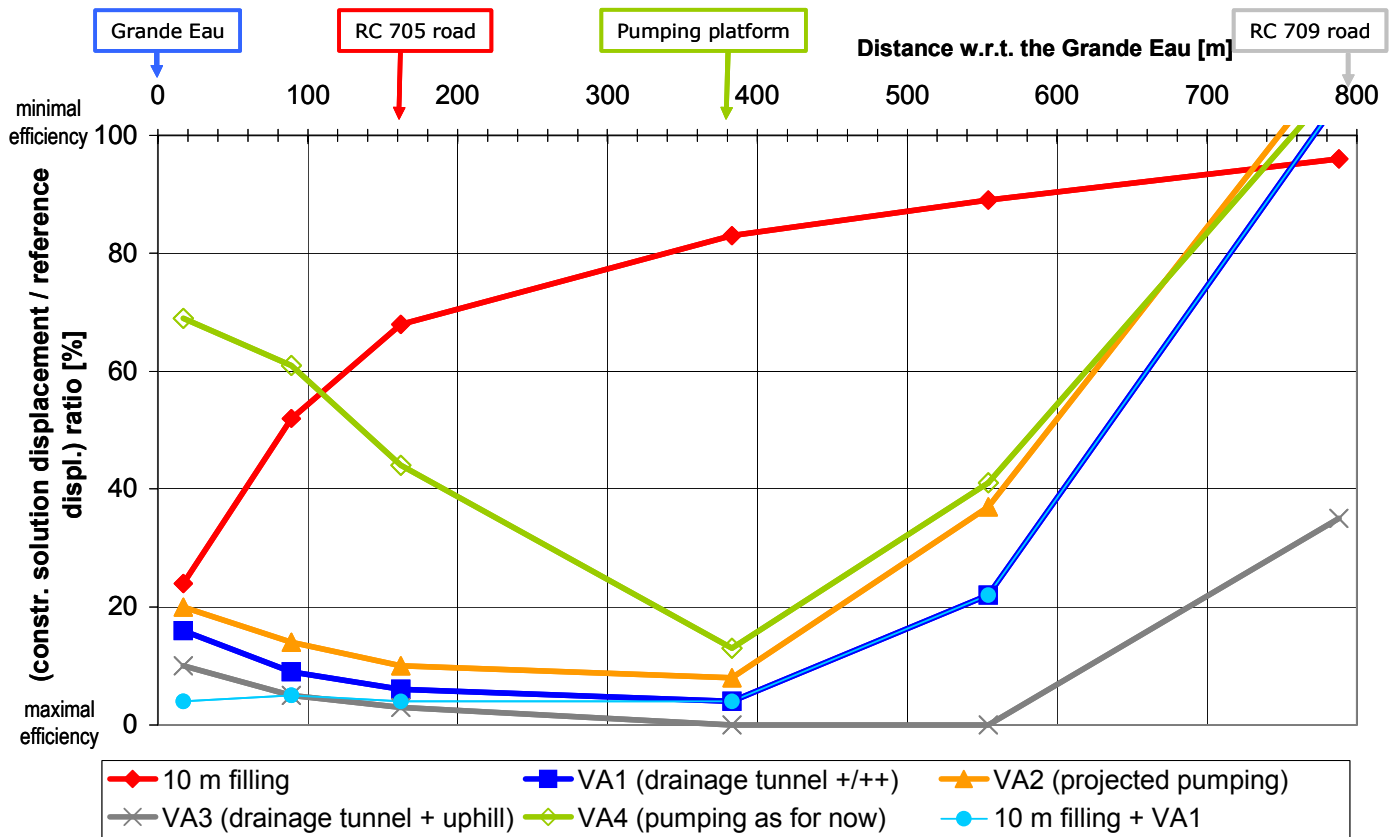


Figure 13. Efficiency of different constructive solutions.

Table 2. Safety factor and potential failure mechanism associated with each constructive solution. Safety analyses are performed at the end of the crisis period, end January 1994.

Case	SF	Critical zone	Case	SF	Critical zone
Reference case	1.05		Drainage tunnel + uphill tunnel (VA3)	1.45	
Filling 10 m	1.20		Existing pumping "as for now" (VA4)	1.05	
Projected drainage tunnel (VA1)	1.30		Projected pumping (VA2)	1.15	